

## Towards a Topological Mechanism of Quark Confinement

Ernst-Michael ILGENFRITZ<sup>1,2</sup>, Harald MARKUM<sup>3</sup>, Michael MÜLLER–PREUSSKER<sup>2</sup>,  
Wolfgang SAKULER<sup>3</sup> and Stefan THURNER<sup>3</sup>

<sup>1</sup>*Institute for Theoretical Physics, University of Kanazawa, Japan*

<sup>2</sup>*Institut für Physik, Humboldt–Universität zu Berlin, Germany*

<sup>3</sup>*Institut für Kernphysik, Technische Universität Wien, Austria*

(Received November 20, 2018)

We report on new analyses of the topological and chiral vacuum structure of four-dimensional QCD on the lattice. Correlation functions as well as visualization of monopole currents in the maximally Abelian gauge emphasize their topological origin and gauge invariant characterization. The (anti)selfdual character of strong vacuum fluctuations is revealed by smoothing. In full QCD, (anti)instanton positions are also centers of the local chiral condensate and quark charge density. Most results turn out generically independent of the action and the cooling/smoothing method.

### §1. Introduction

As a matter of fact, nontrivial topology of non-Abelian gauge fields is a characteristic feature of non-perturbative QCD. An economical principle of nature leads us to expect that its characteristic manifestation, instantons, may play a key role in the still elusive mechanism of confinement, which is a very peculiar property of QCD as well. Instantons appear in a semiclassical path integral quantization of this theory while many people expect that confinement itself is not a semiclassical phenomenon. If there is a linkage, the part taken by the instantons can only be an indirect one. What is the missing link? This question is almost as old as the instanton solution. In a first attempt, after the instanton amplitude had been evaluated by 't Hooft,<sup>1)</sup> Callan, Dashen and Gross<sup>2)</sup> tried to build this bridge in a more abstract way, considering instantons contributing to the non-perturbative running of the QCD coupling constant which, eventually, should give rise to a vacuum that does not support quarks but could enclose color neutral bubbles (hadron bags). In this scenario instantons were topological objects by themselves, but their relation to confinement would be of non-topological nature. The same applies to attempts to obtain the string tension from Wilson loops in an uncorrelated instanton gas.<sup>3)</sup> Both approaches have failed to produce confinement with realistic density and size distribution of instantons. Admittedly, the complicated interactions of the semiclassical objects have been taken into account only in a very crude way. The density and size parameters are more or less known, from the resolution of the axial  $U(1)$  problem via the Witten-Veneziano formula, from low energy hadronic spectroscopy (chiral symmetry breaking) and, with instanton sizes differing within a factor of two, also from lattice investigations addressing directly the topology of gauge field configurations.

For a long time, the conclusion was that instantons are unrelated to confinement. An understanding of confinement seemed decoupled from hadron physics and not

really needed to understand the latter being described exclusively by physics at the instanton scale. Indeed, the topological charge  $Q = \pm 1$  of isolated instantons gives rise to fermionic zero-modes via the Atiyah-Singer index theorem. In a dense liquid of instantons, they are split into a band of quasi-zero-modes. The detailed interaction of instantons, their density and overlap, determines the chiral symmetry breaking and the long-range propagation in light hadronic channels.<sup>4)</sup> From this perspective, confinement appears to be a somewhat esoteric issue.

On the other hand, there is a viable explanation of confinement by an effective dual Abelian Higgs theory,<sup>5)</sup> with the charged scalar field being in the condensed phase, where confinement is realized by an area law of t'Hooft loops instead of Wilson loops. If this scalar field represents, by particle-field duality, magnetic charges of the theory we are studying, then it is tempting to look for signals of their condensation in usual lattice QCD configurations. Various gauges have been tested<sup>6)</sup> to extract *the relevant* degrees of freedom at long distances, being Abelian and giving rise to magnetic charges in an appropriate projection, and to provide evidence for condensation. While the effective action of *this reduced* Abelian gauge field theory coupled to charges and monopoles is probably too complicated to be *effective*, the reduced action of monopoles alone can be put into relation with the above mentioned *dual* Abelian Higgs model.<sup>7)</sup> The phenomenological effective dual Ginzburg-Landau theory can also account for chiral symmetry breaking and restoration.<sup>8)</sup> It seems, that the concept of the dual superconductor mechanism<sup>9)</sup> can be worked out in this framework, and the actual agents of confinement are monopoles with respect to the Abelian subgroup  $U(1)^{N-1}$  of color  $SU(N)$ .

If, in this context, instantons support confinement, they must provide the basic mechanism which helps monopoles to condense. A few years ago, it has been demonstrated that Abelian monopole currents (identified in the maximally Abelian gauge) and topological density are highly correlated quantities, in Monte Carlo ensembles<sup>10)</sup> as well as for instantons and instanton-antiinstanton pairs.<sup>11)</sup> It has been demonstrated that the Abelian monopoles carry also electric charge.<sup>12)</sup> This observation lends support to dyonic vacuum models.<sup>13)</sup> All this has been taken as indication that Abelian monopoles as agents of the confinement mechanism might have a topological origin such that finally both approaches can be united. Reconstructing gauge fields from instanton ensembles identified on genuine lattice gauge field configurations fails to reconstruct the string tension.<sup>14)</sup> Some important parameters characterizing instanton liquids as far as confinement is concerned seem to be unidentified so far. It has been conjectured, that not only instantons but monopoles, too, are related to chiral symmetry breaking.<sup>15)</sup> In contrast to the case of confinement, here is even evidence on the lattice that the reconstruction of gauge fields from the monopole degrees of freedom successfully describes the behavior of the near-to-zero-modes of the fermions.<sup>16)</sup> Chiral symmetry breaking is a collective effect. It seems that the missing information about the large scale structure of the instanton liquid is encoded in the monopole degrees of freedom.

Today, in distinction to the times of the pioneering work by Callan, Dashen and Gross, there exists a multitude of tools within the lattice approach to address afresh the question of confinement due to instantons and to come, hopefully, to a

definite answer. After all, besides all approximate non-perturbative working schemes for (non-supersymmetric) QCD, lattice simulation is the only method based solely on first principles. In this contribution we give further support for the ideas above. We discuss new tools for the investigation of the instanton-confinement issue. We demonstrate the way how instantons and monopoles coexist on individual gauge field configurations, by extracting correlation functions from individual fields and by direct visualization, both in the confinement and in the deconfinement phase. We present selected results obtained by a Wilson renormalization group motivated smoothing method<sup>17),18),19)</sup> and point out the dominance of locally (anti)self dual gauge fields. We report also of new results on local correlations between the quark condensate and the quark charge density on one hand and the topological charge and the local monopole current density on the other, illustrating the mechanism of chiral symmetry breaking.

## §2. Observables and Techniques

There exist several definitions of the Pontryagin number and its density on a Euclidean lattice. One class are the so-called field theoretic definitions which discretize the topological charge density in the continuum,  $q(x) = \frac{g^2}{32\pi^2} \epsilon^{\mu\nu\rho\sigma} \text{Tr} (F_{\mu\nu}(x)F_{\rho\sigma}(x))$ , in the following two ways:<sup>20)</sup>

$$q^{(P,H)}(x) = -\frac{1}{2^4 32\pi^2} \sum_{\mu, \dots = \pm 1}^{\pm 4} \tilde{\epsilon}_{\mu\nu\rho\sigma} \text{Tr} O_{\mu\nu\rho\sigma}^{(P,H)}, \quad (2.1)$$

with

$$O_{\mu\nu\rho\sigma}^{(P)} = U_{\mu\nu}(x)U_{\rho\sigma}(x) \quad (2.2)$$

the plaquette prescription, and by the hypercube prescription

$$\begin{aligned} O_{\mu\nu\rho\sigma}^{(H)} &= U_\mu(x)U_\nu(x+\hat{\mu})U_\rho(x+\hat{\mu}+\hat{\nu})U_\sigma(x+\hat{\mu}+\hat{\nu}+\hat{\rho}) \\ &\times U_\mu^\dagger(x+\hat{\nu}+\hat{\rho}+\hat{\sigma})U_\nu^\dagger(x+\hat{\rho}+\hat{\sigma})U_\rho^\dagger(x+\hat{\sigma})U_\sigma^\dagger(x). \end{aligned} \quad (2.3)$$

Besides of this, there is a geometric definition<sup>21)</sup> where integrals over transition functions between local gauge patches are defining local contributions to the topological charge.

To investigate monopole currents we project  $SU(N)$  onto its Cartan subgroup extracting Abelian degrees of freedom in a way that leaves the Abelian  $U(1)^{N-1}$  gauge symmetry intact. We employ the so-called maximally Abelian gauge.<sup>22)</sup> This gauge is the most likely one to guarantee that the Abelian projection captures long range physics encoded in the gauge field configurations. Monopole charge currents can then be defined on the dual lattice which are both quantized and topologically conserved. For purposes of measuring correlations, the monopole currents  $m(x, \mu)$  are locally summed into a rotational invariant monopole density

$$\rho_m(x) = \frac{1}{4} \sum_{\mu} |m(x, \mu)|. \quad (2.4)$$

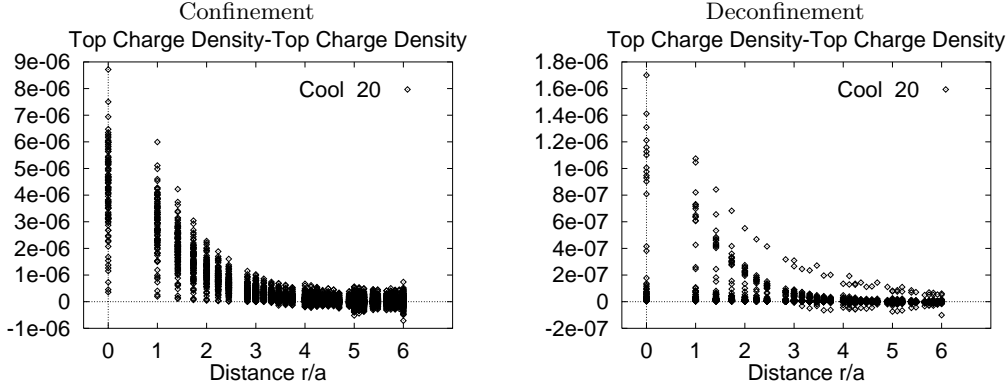


Fig. 1. Correlation functions of the topological charge density in 100 individual configurations representing both phases of pure  $SU(2)$  gauge theory. Measured after 20 cooling steps.

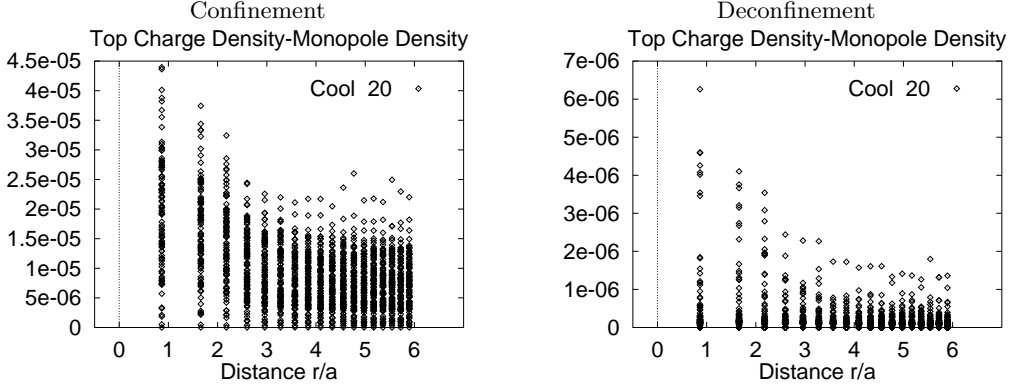


Fig. 2. The  $\rho_m|q|$ -correlation functions of individual configurations are displayed for both phases. All configurations with nonvanishing  $qq$ -correlation give rise to a nontrivial  $\rho_m|q|$ -correlator.

A local quark condensate can be defined by inverting the fermionic matrix  $M$  of the QCD action and taking the trace over all but the space-time indices of  $M^{-1}$ ,

$$\bar{\psi}\psi(x) \equiv \text{tr}M^{-1}. \quad (2.5)$$

Another observable of interest is the local fermionic charge density

$$\psi^\dagger\psi(x) \equiv \text{tr}\gamma_4 M^{-1}. \quad (2.6)$$

Since topological objects with opposite sign are equally probable in the quantum ensemble, we measure the correlation of the monopole density and the local quark condensate with the absolute values of the topological charge density and of the fermionic charge density.

Some of the correlators require the suppression of ultraviolet quantum fluctuations. In most of our studies we have employed the controlled (small step-size) cooling technique which, when applied to the  $SU(3)$  case, uses the Cabibbo-Marinari method (cooling within the  $SU(2)$  subgroups). In the confinement phase, monitoring the string tension, we keep control to what extent the cooled ensemble still

reproduces the vacuum properties. In the deconfinement phase, the same conditions of mild cooling are applied. Finally, however, the cooling method drives all gauge field configurations into classical configurations. In a theoretically uncontrolled way important physical information like instanton sizes, relative positions and color orientation will be finally erased. Therefore, more recently, we have supplemented our methods by a renormalization group motivated smoothing technique.<sup>18),19)</sup> Being a specific inversion of the block spin transformation from a fine to a coarse lattice, this method aims to reconstruct the smoothest interpolation for any given lattice configuration. This is achieved by a constrained minimization of a classically perfect action. Since the coupling parameters of this action are determined with the help of inverse blocking, this method is theoretically self-consistent. The smoothed configurations conserve the physics at scales above the resolution of the coarser lattice.

### §3. Instantons and Monopoles

Our search for the interrelation between topological charge density and magnetic charge currents in the quantized vacuum starts with the measurement of the correlations between the corresponding operators defined above. Going beyond previous correlation measurements, we have now evaluated the correlation functions for individual configurations, for instance

$$C_{qq}(r) = \frac{1}{L_s^3 L_\tau} \sum_{x,y} q(x)q(y)\delta(r - x + y). \quad (3.1)$$

We have analyzed lattice gauge field configurations created with the pure  $SU(2)$  standard Wilson action on a  $12^3 \times 4$  lattice both in the confinement and deconfinement phase at  $\beta = 2.25$  and  $2.4$ , respectively.

Fig. 1 presents the correlation function of the topological charge  $q(x)$  with itself and Fig. 2 the  $\rho_m|q|$ -correlation function for 100 different configurations. The measurements refer to cooled configurations after 20 cooling steps where in the confinement the string tension of the ensemble still amounts to about 80% of the uncooled string tension. In the confinement phase, the configurations differ strongly in the amplitudes (not in the shapes) of the  $qq$ -correlation functions. This reflects the big width of the multiplicity distribution in the number of instantons and antiinstantons. Also the corresponding correlators between monopole and topological density show many different amplitudes. They decrease towards the nonzero cluster value which is not subtracted and represent the nontrivial charge content of the particular configuration. In the deconfinement phase only approximately 15% of the configurations have nontrivial  $qq$ -correlation functions (an amplitude larger than 10% of the biggest in the sample). All these configurations give rise to a nontrivial  $\rho_m|q|$ -correlation. This illustrates how the correlation between monopoles and topological charge measured previously by averaging over the (cooled or uncooled) quantum ensemble manifests itself for individual configurations. It shows that the amplitude is correlated with the topological activity  $A = \sum_x |q(x)|$  which becomes an approximation for the number of instantons and antiinstantons if the (cooled) configurations are sufficiently smooth. Concerning the shapes of both correlation

functions an additional analysis could clarify whether their approach to the cluster value is exponential with a screening mass eventually depending on the topological content of the configuration.

As an instructive example, we visualize in Fig. 3 the topological charge distribution together with the monopole currents for a configuration with net topological charge  $Q = 0$  taken from the ensemble describing the deconfinement phase. We show clusters of topological charge and the accompanying monopole loops, in two time-slices in the upper row, and in two fixed space-slices in the lower. For any value of the topological charge density  $q(x) > 0.005$  a light dot and for  $q(x) < -0.005$  a dark dot is plotted. Monopole loops are represented by thick lines. This configuration contains only one instanton and one antiinstanton. In the deconfinement phase, monopole loops are purely time-like, almost static and must exist in monopole-antimonopole pairs. Here, each (anti)monopole loop tends to pass through an (anti)instanton which extends throughout all four time-slices. In the confinement phase, such pictures look qualitatively similar except that also space-like monopole currents exist and monopole loops are closed in all Euclidean directions.<sup>10)</sup>

These observations are corroborated by our recent studies using an  $SU(2)$  fixed-point action and a renormalization group based smoothing method<sup>18),19)</sup> instead of cooling. This method allows to study the structure of the Yang-Mills vacuum without cooling artefacts. The truncated fixed-point action is a combination of plaquette and tilted 6-link loops and contains the traces up to the fourth power. Based on the smoothing method we are able to give more detailed evidence for the local correlation of gauge invariant quantities (topological charge density and action density) with the presence of monopole currents.

Fig. 4 shows for smoothed configurations the average occupation number of magnetic monopoles  $\langle m \rangle$  on the 32 nearest dual links as a function of the local action  $s_{site}(x)$  concentrated around a given lattice point. A sample consisting of 50 configurations at  $\beta = 1.4$  in the confinement phase has been analyzed for this plot. Apart from the change in the range of the distribution of the local action values with  $\beta$ , the same dependence is observed in the deconfinement phase. Fig. 4 additionally shows the dependence of the average number of monopole currents on the local topological charge density for the same sample of configurations. There are practically no lattice points with topological density  $|q(x)| > 0.05$ , irrespectively of  $\beta$ . A physically important point is the increase of the average local density of monopole currents from small action density  $s_{site}(x)$  or topological density  $|q(x)|$  and the saturation for larger values of  $s_{site}(x)$  and  $|q(x)|$ , respectively. The increase of the variance with  $s_{site}$  or  $|q|$  reflects the smaller number of lattice points with large action or topological density. These results have been obtained using the maximally Abelian gauge for the Abelian projection and the subsequent localization of the Abelian monopoles. A preliminary study using the so-called Polyakov gauge (diagonalizing the Polyakov loop for all space-time lattice points) indicates that the corresponding Abelian monopoles carry less action.

3-dimensional visualizations like Fig. 3 as well as 2-dimensional contour plots in our recent analysis based on the smoothing method<sup>19)</sup> give clear evidence for clustering of the topological density at a scale of several lattice spacings within

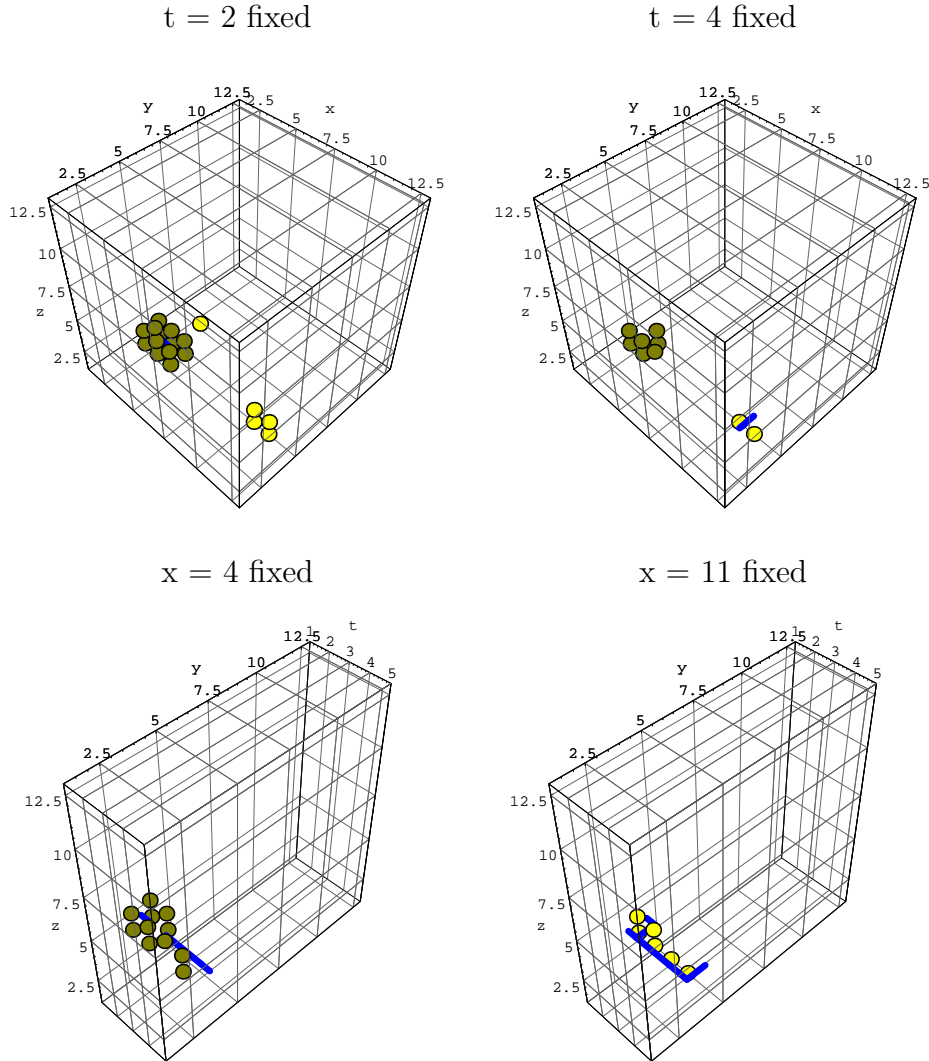


Fig. 3. Two time-slices (upper row) and two fixed space-slices (lower row) visualizing a four-dimensional configuration (after 20 cooling steps) taken from the deconfinement sample, containing an instanton-antiinstanton and a monopole-antimonopole pair. The dots show where the topological charge density  $|q(x)| > 0.005$ . Thick lines represent monopole world lines.

any possible section of the lattice. On the minimally smoothed configurations, reproducing the quantum configurations at any scale above two lattice spacings, the topological density is a continuous function of all Euclidean coordinates. However, a parametrization as classical instantons is hardly possible in the confinement phase if no more sophisticated smoothing techniques<sup>14)</sup> are applied which are biased in some way or another. Taking the action instead of the topological density, the same difficulty is encountered. Nevertheless, one can establish the fact that strong gauge fields are locally nearly selfdual or antiselfdual. A local analysis shows that approxi-

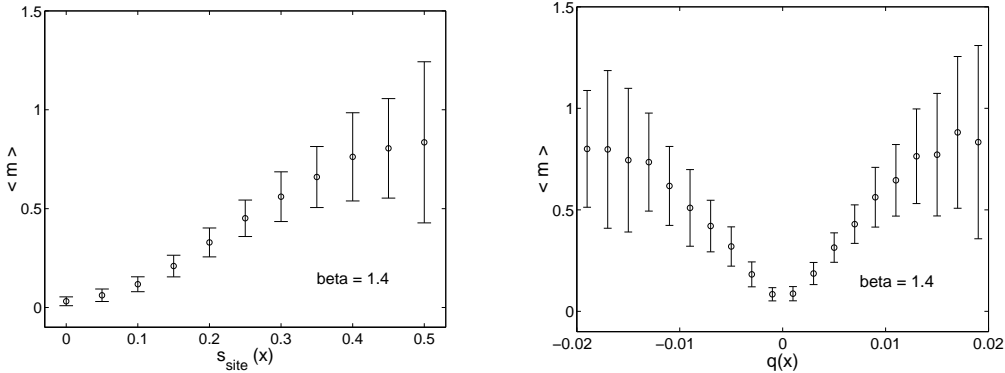


Fig. 4. Average occupation number of magnetic monopoles  $\langle m \rangle$  on the dual links nearest to a lattice point  $x$ , in dependence on the local action  $s_{site}(x)$  (left plot) or the topological density  $q(x)$  (right plot) for minimally smoothed configuration. The figure depicts the situation in the confinement phase at  $\beta = 1.4$ , being similar in the deconfinement phase.

mately selfdual or antiselfdual domains are clearly preferred in both phases when the local action exceeds a threshold value of  $s_{site}(x) \approx 0.3$ . This is demonstrated by the probability distribution of the local topological charge at given local action density in Fig. 5. In other words, smoothing reveals that color-electric and -magnetic fields, if they are strong enough, locally tend to be mutually aligned in color and  $3d$  space. Therefore we must conclude that the (anti)instantons forming a dense fluid become strongly deformed due to interactions and under the influence of quantum fluctuations. We find for all  $\beta$ -values that the (plaquette oriented) topological density is locally bounded by the action density

$$2\pi^2 |q(x)| \leq s_{site}(x). \quad (3.2)$$

This is not unexpected and only confirms that the naive lattice expression (2.2) for the topological charge density is a good operator for smoothed configurations. This is supported also by the correlation between the naive total charge and the geometric charge<sup>18)</sup> giving rise to a charge renormalization factor near to one.

#### §4. Local Chiral Condensate and Quark Charge Density

Here we present results on the correlations of some fermionic observables with the topological density and the monopole density. The simulations have been performed for  $SU(3)$  full QCD with dynamical Kogut-Susskind fermions using the pseudofermionic method on an  $8^3 \times 4$  lattice. The configurations have been generated in the confinement phase at  $\beta = 5.2$  and with 3 flavors of degenerate mass  $m = 0.1$ . When the configurations have been cooled all observables including the fermionic ones have been reevaluated for the ensemble of cooled gauge fields. It must be stressed that cooling here, as in the previous investigations for quenched QCD, denotes a controlled suppression of ultraviolet gluonic quantum fluctuations with respect to the Wilson action, *without* taking the fermionic contribution to the



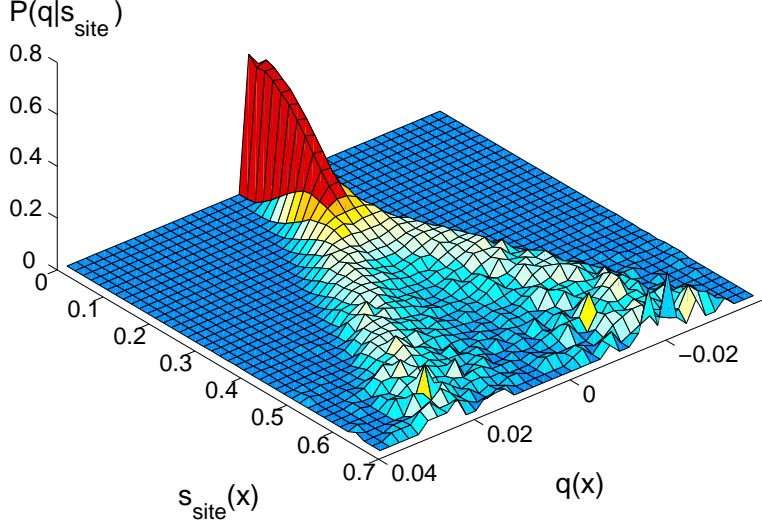


Fig. 5. Probability distributions for finding a local topological charge  $q(x)$  at a lattice site  $x$  where the local action is found to be equal to  $s_{\text{site}}(x)$ . 50 independent confinement configurations obtained for a fixed-point action at  $\beta = 1.4$  have been analyzed and the  $q$  distributions are separately normalized for each value of  $s_{\text{site}}$ .

effective gluonic action into account.

Fig. 6 shows results for connected correlation functions of  $\bar{\psi}\psi(x)$  with  $\rho_m(x)$  and  $q^2(x)$ , averaged over 1000 configurations and normalized at the smallest possible distance. All correlation functions are clearly non-vanishing over distances bigger than two lattice spacings, even for the uncooled ensemble. The correlation of the local quark condensate and the topological charge density is not unexpected,<sup>23)</sup> and

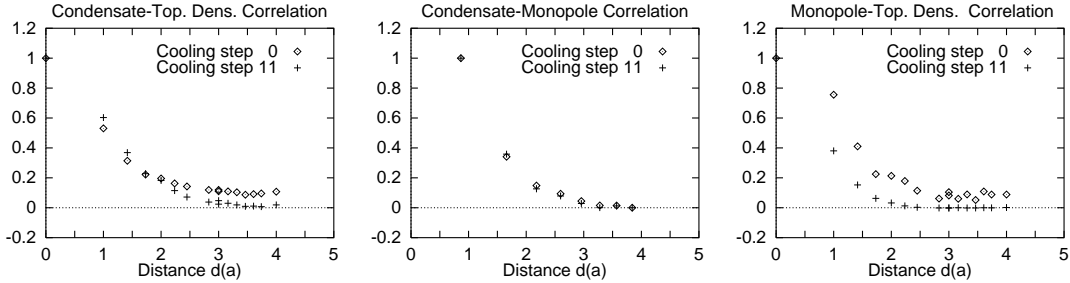


Fig. 6. Correlation functions of the local quark condensate with the topological density squared and with the monopole density (left two plots) and between topological and monopole density. The average is from a non-quenched simulation in the confinement phase. Error bars are comparable to the size of the symbols.

it does not vanish for the largest separations. The long-range correlation becomes reduced with cooling, because fermionic zero-modes of individual instantons start dominating locally in the Kogut-Susskind fermion propagator  $M^{-1}$ .<sup>24)</sup> The correlation between the condensate and the monopole density turns out, however, rather cooling independent whereas the topological-charge monopole correlation decreases slightly with cooling.

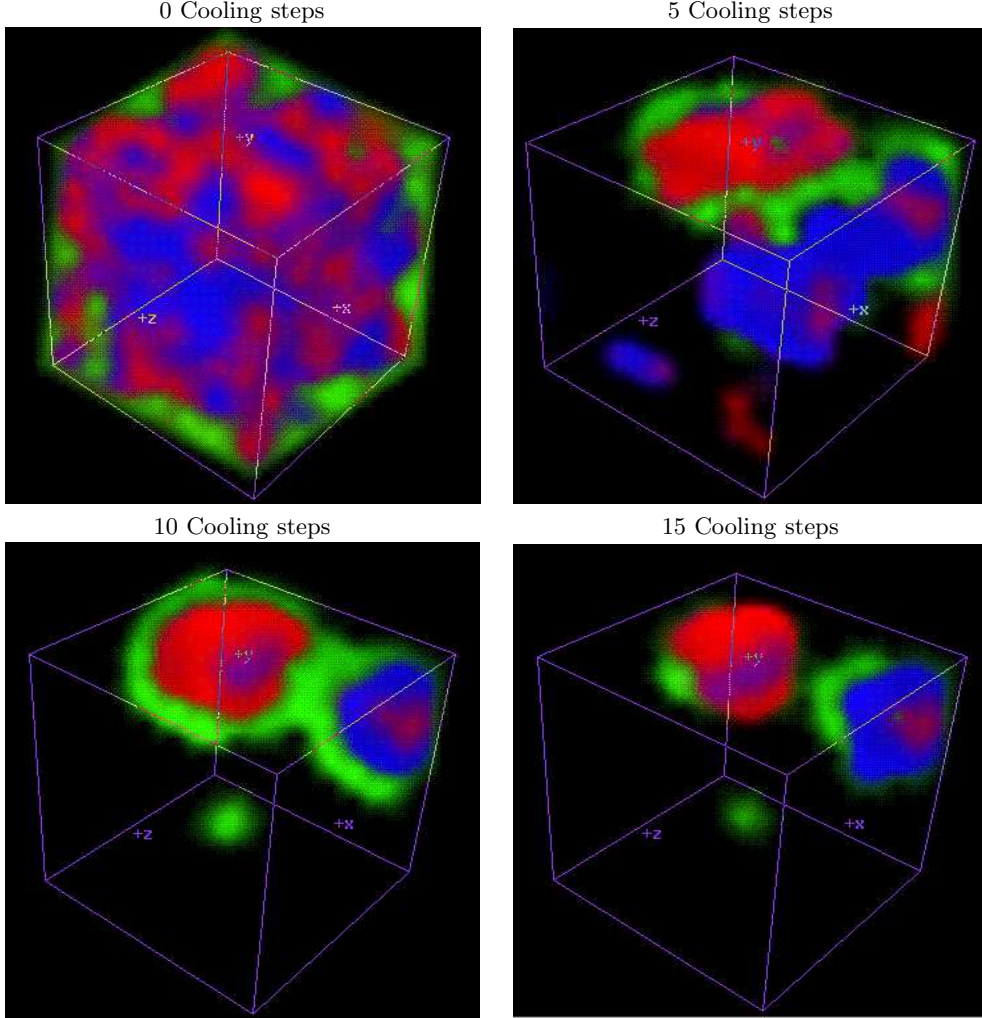


Fig. 7. Cooling history for one time-slice of a gauge field configuration of  $SU(3)$  theory from a non-quenched simulation in the confinement phase. The dark and medium grey shades represent regions of positive and negative topological charge density respectively; the light grey tone surrounding them marks the local quark condensate. See the discussion in the text.

For sufficiently cooled configurations the operator  $\bar{\psi}\psi$  provides an independent measure of the instanton extension and shape. When the topological density profile is given by  $q_\rho(x) \sim \rho^4 (x^2 + \rho^2)^{-4}$  (as for a classical instanton) the corresponding quark zero-mode has a profile  $\bar{\psi}\psi_\rho(x) \sim \rho^2 (x^2 + \rho^2)^{-3}$ . In order to estimate  $\rho$  we

fitted a convolution of the functional form  $C_{\bar{\psi}\psi q}(d) \propto \sum_x \bar{\psi}\psi_\rho(d-x)q_\rho^2(x)$  to our data points. This was evaluated after 11 cooling steps where the configurations are dilute and well-defined instanton sizes can be expected. Our fit yields  $\rho = 1.8$  in lattice spacings. This corresponds to  $\rho \simeq .4$  fm which is consistent with the estimate based on the  $qq$ -correlator. The result is in agreement with other estimates in the literature and supports the conclusion that instantons in the presence of dynamical (sea) quarks are somewhat larger than in pure Yang-Mills theory.

We now visualize the local quark condensate and the topological density on individual gauge field configurations. In Fig. 7 one time-slice of a typical  $SU(3)$  configuration from the non-quenched simulation of the confinement phase is shown. This is a nontrivial  $Q = 0$  configuration containing one instanton-antiinstanton pair. The four pictures illustrate how the extension and shape of the fermionic cloud changes with cooling from the full quantum field theory towards a (semi)classical one. We remind that the fermionic contribution to the gluonic action is neglected in the force driving the gauge field relaxation. We display the region of positive topological density with  $q(x) > 0.003$  by dark grey shades and that with negative density  $q(x) < -0.003$  by a medium grey-tone. The local quark condensate is made visible by a light grey shade whenever a threshold for  $\bar{\psi}\psi(x) > 0.066$  is exceeded. By analyzing dozens of lattice field configurations we found the following picture. The topological charge is hidden by quantum fluctuations and becomes visible only by cooling of the gauge fields. For 0 cooling steps no structure can be seen in  $q(x)$  or  $\bar{\psi}\psi(x)$  on individual configurations. Our results discussed above prove that this does not mean the absence of correlations on the uncooled ensemble. After 5 cooling steps clusters of nonzero topological charge density and local quark condensate are resolved. Both, the localization of the local condensate around instantons and the existence of valence clouds between instantons and antiinstantons, is visible in this stage of cooling. During the next 5 cooling steps the valence cloud of chiral condensate connecting a neighboring instanton-antiinstanton pair becomes gradually weaker. At approximately 10 cooling steps the local quark condensate forms almost separated clouds coinciding with the (anti)instantons. Under further cooling instanton and antiinstanton shrink and finally disappear. Due to the Wilson action they turn into dislocations strongly violating the lattice equation of motion.

Beside the quark condensate  $\bar{\psi}\psi$  the quark charge density  $\psi^\dagger\psi$  represents an interesting quantity. Similarly to QED it reflects the polarization of the QCD vacuum into virtual quarks and antiquarks. The local structure of this polarization cloud and its correlation with topological objects is a challenging issue. Without external sources the net vacuum polarization has to be zero. We know from the previous discussion of  $\bar{\psi}\psi(x)$  that  $\psi^\dagger\psi(x)$  can only be clustered where the topological density clusters. The interesting point is the distribution of the sign of  $\psi^\dagger\psi(x)$ . In Fig. 8 we display a non-quenched  $SU(3)$  configuration on the same lattice size as above. Here a tadpole improved action for the gluons has been used, both for the generation of the (pseudofermionic) Monte Carlo configurations and in the (purely bosonic) cooling. The couplings in the improved bosonic part of the action were chosen to yield approximately the same lattice constant and did not lead to a qualitative change of the physical results described before. After 25 mild cooling sweeps, the

chiral condensate is still seen to be correlated with the topological charge density. The configuration of Fig. 8 consists of a single instanton sitting at the periodic boundary. As expected, the quark charge density is concentrated on the topological cluster. An interesting feature exhibited by the plot, is a characteristic change of sign of  $\psi^\dagger\psi$  inside the domain with  $q(x) \neq 0$ . This gives an insight into the local vacuum polarization mechanism of QCD. Pairs of virtual quarks and antiquarks are created locally predominantly in the regions of nontrivial topology.

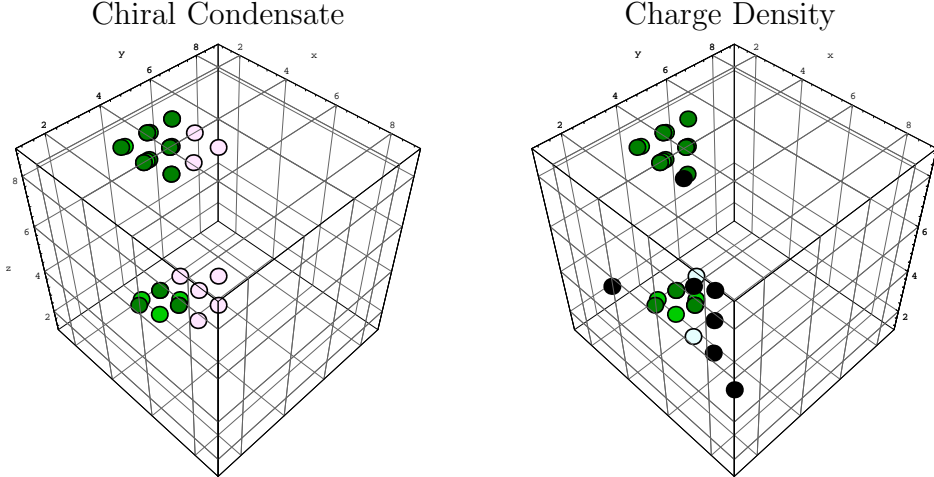


Fig. 8. Comparison of the local chiral condensate and the quark charge density on a non-quenched  $SU(3)$  configuration after 25 cooling steps. The grey dots represent the topological charge density. In the left plot the light dots give the local condensate. In the right plot the dark and light dots show the quark charge density which fluctuates in sign.

## §5. Conclusion

We have calculated the local values of topological charges and monopole currents in the maximally Abelian gauge and directly displayed them with the help of computer graphics. After a few cooling sweeps one observes clearly that instantons are accompanied by monopole loops. We have evidenced that, by averaging over space-time, a nontrivial correlation exists already on individual gauge fields. This is true also in the deconfinement phase although the structure of the monopole currents in this case is completely different from the structure in the confinement phase.

Using a renormalization group based classically perfect action it was shown that, after elimination of quantum fluctuations of  $O(a)$  size by constrained minimization of this action (minimal smoothing), clustering of action and topological charge occurs on a scale of several lattice spacings. These clusters are correlated with monopole currents. After smoothing has been applied it becomes visible that all strong color fields are locally (approximately) selfdual or antiselfdual. However, a parametrization of the smoothed configurations in terms of classical (anti)instantons seems not possible for the dense medium of topological excitations in the confinement phase. Since the smoothed configurations contain relatively few Abelian monopoles the topological

content of the monopole-instanton relation in the Euclidean path integral seems to be accessible for detailed investigation. This is necessary in order to identify the role of instantons for monopole condensation leading to confinement and to point out the role of monopoles for chiral symmetry breaking.

It has turned out that correlations of monopole currents on one hand with the topological density and the local quark condensate on the other are rather insensitive with respect to the cooling or smoothing technique. This, taken together with the result of our visualizations of individual gauge fields, leads us to conjecture that the long distance properties of the topological density distribution of gauge field configurations being relevant for confinement *and* chiral symmetry breaking are encoded in the pattern of monopole currents.

We have further demonstrated the local correlation between instantons (becoming visible by cooling) on one hand and the local quark condensate and the quark charge density on the other. The correlation functions have been evaluated for gauge field configurations from a non-quenched simulation of the confinement phase, before cooling as well as with cooling. For our ensemble of configurations, the correlation function between topological charge density and local condensate has an extent of approximately two lattice spacings which is not very sensitive to the amount of cooling. A fit of this correlation with a convolution of the topological density with  $\bar{\psi}\psi(x)$  leads to an instanton size of about 0.4 fm consistent with other methods. This instanton radius is larger than for quenched  $SU(3)$  gauge theory due to the effect of sea quarks.

As expected, the visualization of the local condensate and the quark charge density shows that both are concentrated to a large extent on top of the (anti)instantons as soon as the latter become identified by cooling. More interesting is what we can learn from the cooling history, showing quantitatively the change of a quantum field to its semiclassical background. When the effect of dynamical quarks is neglected in the gluonic cooling, the valence cloud of chiral condensate connecting a neighboring instanton-antiinstanton pair gradually disappears before, under further cooling, (anti)instantons shrink and dwindle as dislocations. This demonstrates that not just the instantons but also the interpolating gauge field is important for the propagation of quarks on the instanton liquid background. These observations give direct insight into the local interplay of chiral symmetry breaking and nontrivial topological structure. Further examination of the fermionic vacuum structure has exhibited that the quark charge density fluctuates locally giving thus evidence for quark pair creation inside instantons. It must be emphasized that these fermionic results have been obtained on a rather small lattice with finite quark mass. No attempt to extrapolate towards the thermodynamic and chiral limits has been made.

Most of the statistical correlation functions turned out to be generically independent of the smoothing technique and of the choice of the action. This indicates that they are a characteristic also for the quantum ensemble of field configurations.

### Acknowledgments

This work was partially supported by FWF under Contract No. P11456-PHY. S. T. would like to thank M. Feurstein for stimulating discussions. E.-M. I., H. M. and M. M.-P. gratefully acknowledge the kind hospitality of T. Suzuki and all other organizers of the *1997 Yukawa International Seminar (YKIS'97) on Non-Perturbative QCD - Structure of the QCD Vacuum* at the Yukawa Institute for Theoretical Physics of Kyoto University.

### References

- [1] G. 't Hooft, Phys. Rev. **D14** (1976), 3432.
- [2] C. G. Callan, R. Dashen, and D. J. Gross, Phys. Rev. **D17** (1978), 2717; Phys. Rev. **D19** (1979), 1826.
- [3] C. G. Callan, R. Dashen, and D. J. Gross, Phys. Rev. **D18** (1978), 4684.
- [4] T. Schäfer and E. V. Shuryak, Rev. Mod. Phys., in print; e-print archive hep-ph/9610451; E. V. Shuryak, Lecture at this Seminar.
- [5] T. Suzuki, Lecture at this Seminar.
- [6] M. N. Chernodub and M. I. Polikarpov, e-print archive hep-th/9710205 (Lecture at the Workshop "Confinement, Duality and Non-Perturbative Aspects of QCD", Cambridge).
- [7] S. Kato, M. N. Chernodub, S. Kitahara, N. Nakamura, M. I. Polikarpov, and T. Suzuki, e-print archive hep-lat/9709092 (Talk at LATTICE'97); Talks by N. Nakamura and S. Kato at this Seminar.
- [8] S. Sasaki, H. Suganuma, and H. Toki, Phys. Lett. **B387** (1996), 145; H. Toki, Lecture at this Seminar.
- [9] G. 't Hooft, Nucl. Phys. **B190** (1981), 455.  
S. Mandelstam, Phys. Rep. **67** (1980), 109; in Proc. Trieste Monopole Meeting 1981, p. 289.
- [10] S. Thurner, M. Feurstein, H. Markum, and W. Sakuler, Phys. Rev. **D54** (1996), 3457.  
S. Thurner, M. Feurstein, and H. Markum, Phys. Rev. **D56** (1997), 4039.  
M. Feurstein, H. Markum, and S. Thurner, Phys. Lett. **B396** (1997), 203.
- [11] M. N. Chernodub and F. V. Gubarev, JETP Lett. **62** (1995), 100.  
R. C. Brower, K. N. Orginos, and C.-I Tan, Nucl. Phys. **B** (Proc. Suppl.) **53** (1997), 488; Phys. Rev. **D55** (1997), 6313.
- [12] V. Bornyakov and G. Schierholz, Phys. Lett. **B384** (1996), 190.
- [13] Yu. A. Simonov, Lecture at International School of Physics, 'Enrico Fermi', Course 80: Selected Topics in Nonperturbative QCD, Varenna, Italy, p. 339.
- [14] T. DeGrand, A. Hasenfratz, T. G. Kovacs, Nucl. Phys. **B505** (1997), 417; e-print archive hep-lat/9710078; T. DeGrand, Lecture at this Seminar.
- [15] O. Miyamura, Nucl. Phys. **B** (Proc. Suppl.) **42** (1995), 538.
- [16] S. Sasaki and O. Miyamura, e-print archive hep-lat/9706001; e-print archive hep-lat/9709070 (Talk at LATTICE'97); O. Miyamura, Lecture at this Seminar; S. Sasaki, Talk at this Seminar.
- [17] T. DeGrand, A. Hasenfratz, P. Hasenfratz, and F. Niedermayer, Nucl. Phys. **B454** (1995), 578; Nucl. Phys. **B454** (1995), 615.
- [18] M. Feurstein, E.-M. Ilgenfritz, M. Müller-Preussker, and S. Thurner, Nucl. Phys. **B**, in print; e-print archive hep-lat/9611024.
- [19] E.-M. Ilgenfritz, H. Markum, M. Müller-Preussker, and S. Thurner, e-print archive hep-lat/9801040.
- [20] P. Di Vecchia, K. Fabricius, G. C. Rossi, and G. Veneziano, Nucl. Phys. **B192** (1981), 392; Phys. Lett. **B108** (1982), 323; Phys. Lett. **B249** (1990), 490.
- [21] M. Lüscher, Comm. Math. Phys. **85** (1982), 29.  
A. S. Kronfeld, M. L. Laursen, G. Schierholz, and U.-J. Wiese, Nucl. Phys. **B292** (1987), 330.
- [22] A. S. Kronfeld, G. Schierholz, and U.-J. Wiese, Nucl. Phys. **B293** (1987), 461.
- [23] S. J. Hands and M. Teper, Nucl. Phys. **B347** (1990), 819.
- [24] E.-M. Ilgenfritz, M. L. Laursen, M. Müller-Preussker, G. Schierholz, and A. Schiller, Nucl. Phys. **B268** (1986), 693.